

Dexterous Manipulation by Two Fingers with Coupled Joints

Yan-Bin Jia Yuechuan Xue
 Department of Computer Science
 Iowa State University
 Ames, IA 50011, USA
 jia, yuechuan@iastate.edu

Abstract—This paper studies dexterous manipulation in the plane by a two-fingered hand in the plane. The dynamics of each finger, which consists of two links with coupled joints, are derived based on Lagrangian mechanics. As an object is being manipulated, its orientation and the two independent joint angles of the hand constitute the state of the entire system. Contact kinematics, accounting for both stick and slip modes, are combined with dynamics to establish a dependence of the object’s linear and angular accelerations on joint accelerations. This allows control of joint torques, under a proportional-derivative (PD) law, to move the object to a target position in a desired orientation.

I. INTRODUCTION

Industrial robots conventionally adopt independent joint control schemes which are easy to implement, have high failure tolerance, and can provide adequate degrees of freedom for mostly pick-and-place tasks. In the early design of a robotic hand, every finger was equipped with an abundance of actuators to achieve the same number of degrees of freedom (DOFs). For example, the Stanford/JPL hand [13] had three fingers with 3 joints each for a total of 9 DOFs, while the MIT/Utah hand [8] had eight fingers with 4 joints each. Such a hand with high complexities would be difficult for kinematic and dynamic analyses as well as manipulation control. Consequently, later hands were often underactuated using coupled control schemes, resulting in fewer DOFs than joints. Examples include the Barrett Hand [14], of which every finger has two joints but one actuation with a break-away clutch, the anthropomorphic Shadow Hand [12], which is backdrivable with 20 DOFs for 24 joints, and the minimalist SDM Hand [6], which has only 1DOF for all 8 joints.

While underactuated hands can facilitate a range of tasks, their kinematic and dynamic models are rarely provided by the manufacturers or the designers. Investigations by others into such models, as done for the Barrett Hand in [7], are often either brief or detached from real tasks so the work cannot directly benefit the user.

Meanwhile, dexterous manipulation with multifingered hands has mostly focused on the use of rolling contact [5], [2] largely because of the convenience of tracking the position of the manipulated object relative to the hand, and also the avoidance of complications from switching contact modes between stick and slip. Whenever sliding was treated for a robotic hand, it was usually considered alone [10], [4] or based on quasi-static analysis [3]. In [15], sliding was leveraged to lift a planar object off its support to form an enveloping grasp.

In this paper, we will study a simple 2D hand with two fingers, each having two links driven by joints that are coupled under one control. We will investigate the contact kinematics and dynamics for the hand’s manipulation of an object, and present a control of joint torques to re-position and re-orient the object within the hand.

II. FINGER KINEMATICS

As shown in Fig. 1, the hand comprises a horizontal

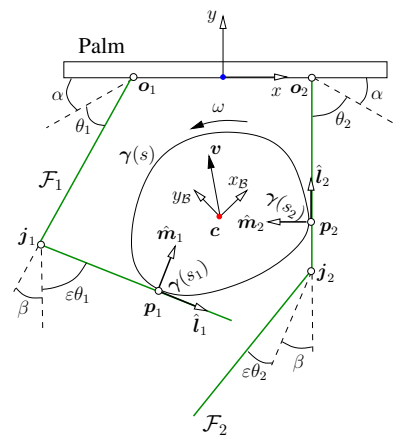


Fig. 1. Two fingers manipulating an object bounded by a curve $\gamma(s)$. palm and two identical fingers \mathcal{F}_1 and \mathcal{F}_2 modeled as

line segments. Each finger \mathcal{F}_i , $i = 1, 2$, has an upper link \mathcal{U}_i and a lower link \mathcal{L}_i with lengths $\ell^{(u)}$ and $\ell^{(l)}$, respectively. The upper link is connected to the palm and the lower link at the joints \mathbf{o}_i and \mathbf{j}_i , and forms initial joint angles $\alpha, \beta > 0$ with them, respectively. Under a coupled movement, the two joint angles always have values $\alpha + \theta_i$ and $\beta + \varepsilon\theta_i$, for some $\theta_i, \varepsilon > 0$. This mimics the movement of a finger of the Barrett Hand [1], driven by a single motor, before any of its fingers makes contact with the object.¹

The hand configuration are thus completely characterized by θ_1 and θ_2 . For uniform treatment of the lower and upper links, we introduce, for $i = 1, 2$,

$$\phi_i = \begin{cases} \alpha + \theta_i, & \text{if upper link } \mathcal{U}_i, \\ \alpha + \beta + (1 + \varepsilon)\theta_i, & \text{if lower link } \mathcal{L}_i. \end{cases} \quad (1)$$

We place the world frame x - y at $(\mathbf{o}_1 + \mathbf{o}_2)/2$ with its x -axis pointing from \mathbf{o}_1 to \mathbf{o}_2 . On the finger \mathcal{F}_i , we let $\hat{\mathbf{m}}_i$ be the unit vector normal to the link and pointing towards the object, and $\hat{\mathbf{l}}_i$ its orthogonal unit vector such that $\hat{\mathbf{l}}_i \times \hat{\mathbf{m}}_i = 1$. Thus,

$$\hat{\mathbf{l}}_i = \begin{pmatrix} -\cos \phi_i \\ \mp \sin \phi_i \end{pmatrix} \quad \text{and} \quad \hat{\mathbf{m}}_i = \begin{pmatrix} \pm \sin \phi_i \\ -\cos \phi_i \end{pmatrix}, \quad (2)$$

where throughout the paper, an operator ‘ \pm ’ or ‘ \mp ’ has its upper sign chosen if $i = 1$ and its lower sign chosen if $i = 2$. The finger joint \mathbf{j}_i has the location

$$\mathbf{j}_i = \mathbf{o}_i + \ell^{(u)} \begin{pmatrix} \mp \cos(\alpha + \theta_i) \\ -\sin(\alpha + \theta_i) \end{pmatrix}. \quad (3)$$

The derivatives $\phi'_i, \hat{\mathbf{l}}'_i, \hat{\mathbf{m}}'_i$ and \mathbf{j}'_i , all with respect to θ_i , can be easily obtained from (1)–(3). In the paper we will use ‘ \prime ’ for differentiation with respect to the (unique) underlying variable, while ‘ $\dot{}$ ’ for differentiation with respect to time.

III. GEOMETRY OF CONTACT

From Fig. 1, the location \mathbf{c} of the object’s center of mass is determined by the joint angles θ_1 and θ_2 and the object’s orientation, described by the rotation angle ψ of its body frame x_B - y_B at \mathbf{c} from the world frame. Introduce two vectors:

$$\boldsymbol{\zeta} = \begin{pmatrix} \theta_1 \\ \theta_2 \\ \psi \end{pmatrix} \quad \text{and} \quad \boldsymbol{\theta} = \begin{pmatrix} \theta_1 \\ \theta_2 \end{pmatrix}.$$

We would like to describe the state of the system by $\boldsymbol{\zeta}$ and its derivative.

¹For the Barrett Hand model BH262, $\varepsilon = \frac{9}{28}$. On contact, its proximal link will be locked while its distal link will start to wrap around the object.

A. Center of Mass

The object is in simultaneous contact with the two fingers \mathcal{F}_1 and \mathcal{F}_2 at the points \mathbf{p}_1 and \mathbf{p}_2 , respectively. For $i = 1, 2$ define

$$\boldsymbol{\delta}_i = \begin{cases} \mathbf{o}_i, & \text{if } \mathbf{p}_i \text{ on } \mathcal{U}_i, \\ \mathbf{j}_i, & \text{if } \mathbf{p}_i \text{ on } \mathcal{L}_i. \end{cases} \quad (4)$$

Let d_i be the distance from the joint $\boldsymbol{\delta}_i$ to \mathbf{p}_i . Then,

$$\mathbf{p}_i = \boldsymbol{\delta}_i \pm d_i \hat{\mathbf{l}}_i. \quad (5)$$

For $i = 1, 2$ we let r_i be the distances from \mathbf{c} to \mathbf{p}_i . Depending on $\boldsymbol{\zeta}$, expressions for r_1 and r_2 can be derived. We have

$$(\mathbf{c} - \boldsymbol{\delta}_i) \cdot \hat{\mathbf{m}}_i = r_i, \quad i = 1, 2.. \quad (6)$$

Since $\hat{\mathbf{l}}_1$ and $\hat{\mathbf{m}}_1$ are orthogonal, we decompose $\hat{\mathbf{m}}_2$ as $\hat{\mathbf{m}}_2 = (\hat{\mathbf{m}}_2 \cdot \hat{\mathbf{l}}_1)\hat{\mathbf{l}}_1 + (\hat{\mathbf{m}}_2 \cdot \hat{\mathbf{m}}_1)\hat{\mathbf{m}}_1$, and take the dot products of \mathbf{c} with both sides:

$$\mathbf{c} \cdot \hat{\mathbf{m}}_2 = (\hat{\mathbf{m}}_2 \cdot \hat{\mathbf{l}}_1)(\mathbf{c} \cdot \hat{\mathbf{l}}_1) + (\hat{\mathbf{m}}_2 \cdot \hat{\mathbf{m}}_1)(\mathbf{c} \cdot \hat{\mathbf{m}}_1),$$

from which we obtain

$$\mathbf{c} \cdot \hat{\mathbf{l}}_1 = \frac{\mathbf{c} \cdot \hat{\mathbf{m}}_2 - (\hat{\mathbf{m}}_1 \cdot \hat{\mathbf{m}}_2)(\mathbf{c} \cdot \hat{\mathbf{m}}_1)}{\hat{\mathbf{l}}_1 \cdot \hat{\mathbf{m}}_2}.$$

Hence,

$$\begin{aligned} \mathbf{c} &= (\mathbf{c} \cdot \hat{\mathbf{l}}_1)\hat{\mathbf{l}}_1 + (\mathbf{c} \cdot \hat{\mathbf{m}}_1)\hat{\mathbf{m}}_1 \\ &= \frac{(\mathbf{c} \cdot \hat{\mathbf{m}}_2)\hat{\mathbf{l}}_1 - (\mathbf{c} \cdot \hat{\mathbf{m}}_1)(\hat{\mathbf{m}}_2 \times (\hat{\mathbf{l}}_1 \times \hat{\mathbf{m}}_1))}{\hat{\mathbf{l}}_1 \cdot \hat{\mathbf{m}}_2} \\ &= \frac{(\boldsymbol{\delta}_2 \cdot \hat{\mathbf{m}}_2 + r_2)\hat{\mathbf{l}}_1 - (\boldsymbol{\delta}_1 \cdot \hat{\mathbf{m}}_1 + r_1)\hat{\mathbf{l}}_2}{\hat{\mathbf{l}}_1 \cdot \hat{\mathbf{m}}_2}, \end{aligned} \quad (7)$$

where the last step utilized $\hat{\mathbf{m}}_2 \times (\hat{\mathbf{l}}_1 \times \hat{\mathbf{m}}_1) = \hat{\mathbf{l}}_2$, and then plugged in (6).

Differentiations of \mathbf{c} yield the object’s velocity and acceleration:

$$\mathbf{v} = \left(\frac{\partial \mathbf{c}}{\partial \theta_1}, \frac{\partial \mathbf{c}}{\partial \theta_2}, \frac{\partial \mathbf{c}}{\partial \psi} \right) \dot{\boldsymbol{\zeta}}, \quad (8)$$

$$\dot{\mathbf{v}} = \left(\frac{\partial \mathbf{c}}{\partial \theta_1}, \frac{\partial \mathbf{c}}{\partial \theta_2} \right) \ddot{\boldsymbol{\theta}} + \frac{\partial \mathbf{c}}{\partial \psi} \ddot{\psi} + \mathbf{a}(\boldsymbol{\zeta}, \dot{\boldsymbol{\zeta}}), \quad (9)$$

where

$$\begin{aligned} \mathbf{a}(\boldsymbol{\zeta}, \dot{\boldsymbol{\zeta}}) &= \frac{\partial^2 \mathbf{c}}{\partial \theta_1^2} \dot{\theta}_1^2 + \frac{\partial^2 \mathbf{c}}{\partial \theta_2^2} \dot{\theta}_2^2 + \frac{\partial^2 \mathbf{c}}{\partial \psi^2} \dot{\psi}^2 + 2 \frac{\partial^2 \mathbf{c}}{\partial \theta_1 \partial \theta_2} \dot{\theta}_1 \dot{\theta}_2 \\ &\quad + 2 \frac{\partial^2 \mathbf{c}}{\partial \theta_1 \partial \psi} \dot{\theta}_1 \dot{\psi} + 2 \frac{\partial^2 \mathbf{c}}{\partial \theta_2 \partial \psi} \dot{\theta}_2 \dot{\psi}. \end{aligned} \quad (10)$$

B. Contact Location

Under the body frame at \mathbf{c} , the object is bounded by a twice differentiable curve $\gamma(s)$ parametrized with arc length s . Every point on the curve has a unit tangent $\hat{\mathbf{t}}(s) = \gamma'(s)$ and a unit normal $\hat{\mathbf{n}}(s)$ such that $\hat{\mathbf{t}}(s) \times \hat{\mathbf{n}}(s) = 1$. The contact points \mathbf{p}_1 and \mathbf{p}_2 are located as $\gamma(s_1)$ and $\gamma(s_2)$, respectively. Given θ_1, θ_2 , and ψ , s_i , $i = 1, 2$, is determined from solving the equation below:

$$\hat{\mathbf{m}}_i(\theta_i) \cdot \left(R(\psi) \hat{\mathbf{t}}(s_i) \right) = 0, \quad (11)$$

where $R(\psi)$ is the rotation matrix of the body frame relative to the world frame. The distances from \mathbf{c} to the two links are

$$r_i = -\gamma(s_i) \cdot \hat{\mathbf{n}}(s_i). \quad (12)$$

For simplicity, we write $\gamma_i = \gamma(s_i)$, $\hat{\mathbf{t}}_i = \hat{\mathbf{t}}(s_i)$, $\hat{\mathbf{n}}_i = \hat{\mathbf{n}}(s_i)$, and $\kappa_i = \kappa(s_i)$, where κ is the curvature function of the curve γ .

The nine partial derivatives of \mathbf{c} needed for evaluating the object's velocity (8) and acceleration (9) can be obtained from differentiating (7). This requires the partial derivatives of r_1 and r_2 , which in turn depend on those of s_1 and s_2 by (12). Differentiating (11) with respect to ψ , θ_1 , and θ_2 , we obtain

$$\frac{\partial s_i}{\partial \psi} = -\frac{\hat{\mathbf{m}}_i \cdot (R'(\psi) \hat{\mathbf{t}}_i)}{\kappa_i} \text{ and } \frac{\partial s_i}{\partial \theta_j} = \begin{cases} \pm \frac{2r_i}{\kappa_i} & \text{if } i = j, \\ 0 & \text{if } i \neq j, \end{cases}$$

where $\eta_i = 1$ if \mathbf{p}_i on \mathcal{U}_i and $\eta_i = 1 + \varepsilon$ if \mathbf{p}_i on \mathcal{L}_i . The second order partial derivatives of s_i are obtained from differentiating (11) twice.

IV. CONTACT FORCE

The object with mass m is subject to two contact forces $\mathbf{f}_i = f_{il} \hat{\mathbf{l}}_i + f_{im} \hat{\mathbf{m}}_i$ yielded by the fingers \mathcal{F}_i , $i = 1, 2$. Newton's and Euler's equations are as follows:

$$m\dot{\mathbf{v}} = \mathbf{f}_1 + \mathbf{f}_2 + m\mathbf{g}, \quad (13)$$

$$\rho\dot{\boldsymbol{\omega}} = -r_1 \hat{\mathbf{m}}_1 \times \mathbf{f}_1 - r_2 \hat{\mathbf{m}}_2 \times \mathbf{f}_2, \quad (14)$$

where ρ is the object's moment of inertia, and $\boldsymbol{\omega} = \dot{\boldsymbol{\phi}}$ its angular velocity. From Euler's equation follows the angular acceleration:

$$\ddot{\boldsymbol{\psi}} = \dot{\boldsymbol{\omega}} = \frac{1}{\rho} (r_1 f_{1l} + r_2 f_{2l}). \quad (15)$$

Below we will apply contact mode analysis to describe \mathbf{f}_1 and \mathbf{f}_2 in terms of $\boldsymbol{\theta}, \dot{\boldsymbol{\theta}}, \ddot{\boldsymbol{\theta}}, \psi$, and $\dot{\psi}$, so the forces can be incorporated into the finger dynamics for object control later in Section V.

Each contact \mathbf{p}_i can be viewed as two coinciding points $\mathbf{p}_i^{(f)}$ and $\mathbf{p}_i^{(o)}$, fixed on the finger \mathcal{F}_i and the

object, respectively. The velocity of $\mathbf{p}_i^{(f)}$ is obtained from differentiating (5) while treating d_i as constant:

$$\mathbf{v}_i^{(f)} = \dot{\boldsymbol{\delta}}_i \pm d_i \dot{\hat{\mathbf{l}}}_i = \boldsymbol{\delta}'_i \dot{\boldsymbol{\theta}}_i + d_i \eta_i \hat{\mathbf{m}}_i \dot{\boldsymbol{\theta}}_i. \quad (16)$$

The velocity of $\mathbf{p}_i^{(o)}$ is

$$\mathbf{v}_i^{(o)} = \mathbf{v} - \dot{\psi} (\boldsymbol{\gamma}_i \cdot \hat{\mathbf{n}}_i) \hat{\mathbf{l}}_i. \quad (17)$$

A. Sliding

Both contacts \mathbf{p}_1 and \mathbf{p}_2 are sliding. The sign of $(\mathbf{v}_i^{(o)} - \mathbf{v}_i^{(f)}) \cdot \hat{\mathbf{l}}_i$ determines the direction of sliding on \mathcal{F}_i . Introduce

$$\sigma_i = \begin{cases} -1 & \text{if } \mathbf{p}_i \text{ moves in the direction } \hat{\mathbf{l}}_i, \\ 1 & \text{if } \mathbf{p}_i \text{ moves opposite the direction } \hat{\mathbf{l}}_i. \end{cases}$$

Under Coulomb's law of friction, $f_{il} = \mu \sigma_i f_{im}$, where μ is the coefficient of friction. Consequently, equation (15) becomes

$$\ddot{\boldsymbol{\psi}} = \frac{\mu}{\rho} (r_1 \sigma_1 f_{1m} + r_2 \sigma_2 f_{2m}).$$

Substitute the above into (9):

$$\dot{\mathbf{v}} = \left(\frac{\partial \mathbf{c}}{\partial \theta_1}, \frac{\partial \mathbf{c}}{\partial \theta_2} \right) \ddot{\boldsymbol{\theta}} + \frac{\mu}{\rho} \frac{\partial \mathbf{c}}{\partial \psi} \begin{pmatrix} r_1 \sigma_1 \\ r_2 \sigma_2 \end{pmatrix}^T \begin{pmatrix} f_{1m} \\ f_{2m} \end{pmatrix} + \mathbf{a}. \quad (18)$$

The two contact forces are represented as

$$\mathbf{f}_i = f_{im} \mathbf{w}_i, \quad (19)$$

where $\mathbf{w}_i = \hat{\mathbf{m}}_i + \mu \sigma_i \hat{\mathbf{l}}_i$. In Newton's equation (13), we move $m\mathbf{g}$ to the left hand side, and then take the dot products of both sides separately with $\hat{\mathbf{m}}_1$ and $\hat{\mathbf{m}}_2$:

$$m(\dot{\mathbf{v}} - \mathbf{g}) \cdot \hat{\mathbf{m}}_1 = f_{1m} + f_{2m} \hat{\mathbf{m}}_1 \cdot \mathbf{w}_2,$$

$$m(\dot{\mathbf{v}} - \mathbf{g}) \cdot \hat{\mathbf{m}}_2 = f_{1m} \hat{\mathbf{m}}_2 \cdot \mathbf{w}_1 + f_{2m}.$$

Solve the above two equations:

$$\begin{pmatrix} f_{1m} \\ f_{2m} \end{pmatrix} = mA^{-1} (\hat{\mathbf{m}}_1, \hat{\mathbf{m}}_2)^T (\dot{\mathbf{v}} - \mathbf{g}), \quad (20)$$

where

$$A = \begin{pmatrix} 1 & \hat{\mathbf{m}}_1 \cdot \mathbf{w}_2 \\ \hat{\mathbf{m}}_2 \cdot \mathbf{w}_1 & 1 \end{pmatrix}. \quad (21)$$

Let

$$L = I_2 - \frac{\mu m}{\rho} A^{-1} (\hat{\mathbf{m}}_1, \hat{\mathbf{m}}_2)^T \frac{\partial \mathbf{c}}{\partial \psi} (r_1 \sigma_1, r_2 \sigma_2), \quad (22)$$

where I_2 is the 2×2 identity matrix. We substitute (18) into (20) to obtain

$$\begin{pmatrix} f_{1m} \\ f_{2m} \end{pmatrix} = K(\boldsymbol{\zeta}) \ddot{\boldsymbol{\theta}} + \mathbf{k}_1(\boldsymbol{\zeta}, \dot{\boldsymbol{\zeta}}) + \mathbf{k}_2(\boldsymbol{\zeta}), \quad (23)$$

where

$$K(\boldsymbol{\zeta}) = mL^{-1} A^{-1} (\hat{\mathbf{m}}_1, \hat{\mathbf{m}}_2)^T \frac{\partial \mathbf{c}}{\partial \boldsymbol{\theta}}, \quad (24)$$

$$\mathbf{k}_1(\boldsymbol{\zeta}, \dot{\boldsymbol{\zeta}}) = mL^{-1} A^{-1} (\hat{\mathbf{m}}_1, \hat{\mathbf{m}}_2)^T \mathbf{a}, \quad (25)$$

$$\mathbf{k}_2(\boldsymbol{\zeta}) = -mL^{-1} A^{-1} (\hat{\mathbf{m}}_1, \hat{\mathbf{m}}_2)^T \mathbf{g}. \quad (26)$$

B. Rolling

Suppose rolling happens at the contact point \mathbf{p}_i with the finger \mathcal{F}_i . Substitute (16) and (17) into $\mathbf{v}_i^{(o)} = \mathbf{v}_i^{(f)}$, and take separate dot products with $\hat{\mathbf{l}}_i$ and $\hat{\mathbf{m}}_i$:

$$\mathbf{v} \cdot \hat{\mathbf{m}}_i = (\delta'_i \cdot \hat{\mathbf{m}}_i + d_i \eta_i) \dot{\theta}_i, \quad (27)$$

$$\mathbf{v} \cdot \hat{\mathbf{l}}_i - \dot{\psi}(\gamma_i \cdot \hat{\mathbf{n}}_i) = (\delta'_i \cdot \hat{\mathbf{l}}_i) \dot{\theta}_i. \quad (28)$$

Can the object be rolling simultaneously on the other finger \mathcal{F}_j , $j \neq i$? Suppose this happens. Then the four equations (27) and (28), for $i = 1, 2$, must hold simultaneously. Substitutions of (8) into them yields four linear equations in three indeterminates: $\dot{\theta}_1$, $\dot{\theta}_2$, and $\dot{\psi}$. Non-trivial values of these indeterminates satisfy the four equations only if the coefficient matrix vanishes, which can happen for no more than a finite number of configurations determined by $(\theta_1, \theta_2, \psi)$. Therefore, simultaneous rolling cannot happen over a non-zero period of time.

From (28) follows the object's angular velocity and acceleration:

$$\dot{\psi} = \frac{\mathbf{v} \cdot \hat{\mathbf{l}}_i - (\delta'_i \cdot \hat{\mathbf{l}}_i) \dot{\theta}_i}{\gamma_i \cdot \hat{\mathbf{n}}_i}, \quad (29)$$

$$\ddot{\psi} = \frac{\kappa_i \dot{s}_i \gamma_i \cdot \mathbf{t}_i}{\gamma_i \cdot \hat{\mathbf{n}}_i} \dot{\psi} + \frac{1}{\gamma_i \cdot \hat{\mathbf{n}}_i} \left(\dot{\mathbf{v}} \cdot \hat{\mathbf{l}}_i + (\mathbf{v} \cdot \hat{\mathbf{l}}_i) \dot{\theta}_i - (\delta''_i \cdot \hat{\mathbf{l}}_i + \delta_i \cdot \hat{\mathbf{l}}_i) \dot{\theta}_i^2 - (\delta'_i \cdot \hat{\mathbf{l}}_i) \ddot{\theta}_i \right), \quad (30)$$

For convenience, let us denote $\phi = \begin{pmatrix} \theta_i \\ \dot{\theta}_i \end{pmatrix}$. We plug (8), (9), and (29) into (30) to solve for $\ddot{\psi}$:

$$\ddot{\psi} = e(\zeta) \cdot \ddot{\phi} + e_1(\zeta, \dot{\zeta}), \quad (31)$$

where

$$e(\zeta) = \left(\gamma_i \cdot \hat{\mathbf{n}}_i - \frac{\partial \mathbf{c}}{\partial \psi} \cdot \hat{\mathbf{l}}_i \right)^{-1} \left(\frac{\partial \mathbf{c}}{\partial \theta_i} - \delta'_i \cdot \hat{\mathbf{l}}_i, \frac{\partial \mathbf{c}}{\partial \theta_j} \right)^T \hat{\mathbf{l}}_i, \\ e_1(\zeta, \dot{\zeta}) = \left(\gamma_i \cdot \hat{\mathbf{n}}_i - \frac{\partial \mathbf{c}}{\partial \psi} \cdot \hat{\mathbf{l}}_i \right)^{-1} \left(\kappa_i \dot{s}_i (\gamma_i \cdot \mathbf{t}_i) \dot{\psi} + \mathbf{a} \cdot \hat{\mathbf{l}}_i + (\mathbf{v} \cdot \hat{\mathbf{l}}_i) \dot{\theta}_i - (\delta''_i \cdot \hat{\mathbf{l}}_i + \delta_i \cdot \hat{\mathbf{l}}_i) \dot{\theta}_i^2 \right).$$

The acceleration (9), with (31) substituted in, becomes $\dot{\mathbf{v}} = D\ddot{\phi} + \mathbf{d}$, where

$$D = \frac{\partial \mathbf{c}}{\partial \phi} + \frac{\partial \mathbf{c}}{\partial \psi} e^T \quad \text{and} \quad \mathbf{d} = e_1 \frac{\partial \mathbf{c}}{\partial \psi} + \mathbf{a}. \quad (32)$$

The other contact \mathbf{p}_j must be sliding. We have $f_{jl} = \mu \sigma_j f_{jm}$, and

$$\mathbf{f}_j = f_{jm} \mathbf{w}_j, \quad (33)$$

where $\mathbf{w}_j = \hat{\mathbf{m}}_j + \mu \sigma_j \hat{\mathbf{l}}_j$. Euler's equation (15) becomes $\ddot{\psi} = \frac{1}{\rho} (r_i f_{il} + r_j \mu \sigma_j f_{jm})$. Equate it with (31):

$$r_i f_{il} + r_j \mu \sigma_j f_{jm} = \rho (e \cdot \ddot{\phi} + e_1). \quad (34)$$

Meanwhile, plug (33) into Newton's equation (13):

$$\mathbf{f}_i = m(\dot{\mathbf{v}} - \mathbf{g}) - f_{jm} \mathbf{w}_j, \quad (35)$$

whose both sides are taken dot products with $\hat{\mathbf{l}}_i$ to yield

$$f_{il} + (\hat{\mathbf{l}}_i \cdot \mathbf{w}_j) f_{jm} = m \hat{\mathbf{l}}_i \cdot (\dot{\mathbf{v}} - \mathbf{g}), \quad (36)$$

From (34) and (36) we obtain, after plugging in (9),

$$f_{jm} = \mathbf{b}(\zeta) \cdot \ddot{\phi} + b_1(\zeta, \dot{\zeta}) + b_2(\zeta), \quad (37)$$

where

$$\mathbf{b}(\zeta) = \frac{1}{r_i \hat{\mathbf{l}}_i \cdot \mathbf{w}_j - r_j \mu \sigma_j} (m r_i D^T \hat{\mathbf{l}}_i - \rho \mathbf{e}), \quad (38)$$

$$b_1(\zeta, \dot{\zeta}) = \frac{m r_i \hat{\mathbf{l}}_i \cdot \mathbf{d} - \rho e_1}{r_i \hat{\mathbf{l}}_i \cdot \mathbf{w}_j - r_j \mu \sigma_j}, \quad (39)$$

$$b_2(\zeta) = -\frac{m r_i \hat{\mathbf{l}}_i \cdot \mathbf{g}}{r_i \hat{\mathbf{l}}_i \cdot \mathbf{w}_j - r_j \mu \sigma_j}. \quad (40)$$

Subsequently, (33) and (35) can be rewritten as

$$\mathbf{f}_k = B_k(\zeta) \ddot{\phi} + \mathbf{s}_k(\zeta, \dot{\zeta}) + \mathbf{t}_k(\zeta), \quad k = i, j, \quad (41)$$

where

$$B_j(\zeta) = \mathbf{w}_j \mathbf{b}^T, \quad B_i(\zeta) = mD - \mathbf{w}_j \mathbf{b}^T, \\ \mathbf{s}_j(\zeta, \dot{\zeta}) = b_1 \mathbf{w}_j, \quad \mathbf{s}_i(\zeta, \dot{\zeta}) = m\mathbf{d} - b_1 \mathbf{w}_j, \\ \mathbf{t}_j(\zeta) = b_2 \mathbf{w}_j, \quad \mathbf{t}_i(\zeta) = -m\mathbf{g} - b_2 \mathbf{w}_j.$$

C. Two Instances

Suppose that the object is a disk with radius r . Its moment of inertia is $\rho = \frac{1}{2} m r^2$. Its center of mass \mathbf{c} has the same distance to the two contacting links: $r_1 = r_2 = r$. By (7), \mathbf{c} is independent of the disk's rotation angle ψ , leading to

$$\frac{\partial \mathbf{c}}{\partial \psi} = \frac{\partial^2 \mathbf{c}}{\partial^2 \psi} = \frac{\partial^2 \mathbf{c}}{\partial \psi \partial \theta_1} = \frac{\partial^2 \mathbf{c}}{\partial \psi \partial \theta_2} = \mathbf{0}. \quad (42)$$

When both contacts are sliding, the matrix $L = I_2$. It is easy to verify that the contact forces \mathbf{f}_i and \mathbf{f}_j are independent of ψ or its derivative (both obtained from integrations of (15)). When the contact \mathbf{p}_i is rolling, the angular velocity $\dot{\psi}$ is given in (29). It is thus independent of ψ , so are the terms D , \mathbf{d} , \mathbf{b} , and for $k = 1, 2$, b_k , B_k , \mathbf{s}_k , \mathbf{t}_k , and finally, \mathbf{f}_i and \mathbf{f}_j .

Suppose that the object is polygonal with n vertices $\mathbf{z}_1, \mathbf{z}_2, \dots, \mathbf{z}_n$, whose coordinates are given in its body frame. Although the boundary is not twice differentiable, modeling can be done with some changes. Every contact point γ_i is some vertex \mathbf{z}_j at the location $R(\psi) \mathbf{z}_j + \mathbf{c}$. As long as the two contact vertices do not change, we evaluate all nine first and second order partial derivatives of \mathbf{c} with respect to θ_1, θ_2 , and ψ . The tangent \mathbf{t}_i and normal $\hat{\mathbf{n}}_i$ at the point need to be replaced with $R \hat{\mathbf{l}}_i$

and $R\hat{\mathbf{m}}_i$ so that differentiations are with respect to the orientation ψ rather than the arc length s .

Transition from a contact vertex \mathbf{z}_j to its adjacent vertex, say, \mathbf{z}_{j+1} , happens at the moment when the edge $\overline{\mathbf{z}_j\mathbf{z}_{j+1}}$ is aligned with the contact link of some finger \mathcal{F}_i . The vertex \mathbf{z}_{j+1} generally has a non-zero normal contact velocity relative to the link. This will result in an impact to cause discontinuities in the object's velocities \mathbf{v} and ω . To cope with this issue, we regard the mass of the hand to be significantly greater than that of the object, and avoid full-scale impact modeling with friction [9]. Let the velocity component $\mathbf{v} \cdot \hat{\mathbf{l}}_i$ not change during the impact but the component $\mathbf{v} \cdot \hat{\mathbf{m}}_i$ change to satisfy (27) to prevent penetration.² This determines the change in velocity $\Delta\mathbf{v}$ and the impulse $m\Delta\mathbf{v}$ on the object. The change in the angular velocity is then $(R\mathbf{z}_j) \times (m\Delta\mathbf{v})/\rho$.

V. DYNAMICS OF MANIPULATION

We will first apply Lagrange mechanics to derive the dynamic equation for a single finger. Then we will combine the equations for both fingers of the hand into one describing the joint torques.

A. Finger Dynamics

Let us go back to Fig. 1. The mass and moment of inertia³ of the upper link of a finger are denoted $m^{(u)}$ and $\rho^{(u)}$, and those of the lower link are denoted $m^{(l)}$ and $\rho^{(l)}$. For $i = 1, 2$, we let $\hat{\mathbf{l}}_i^{(u)}$ and $\hat{\mathbf{m}}_i^{(u)}$ be the vector values assumed by $\hat{\mathbf{l}}_i$ and $\hat{\mathbf{m}}_i$ as given by (2) for the upper link \mathcal{U}_i , and $\hat{\mathbf{l}}_i^{(l)}$ and $\hat{\mathbf{m}}_i^{(l)}$ be their vector values for the lower link \mathcal{L}_i . Let $h^{(u)}$ and $h^{(l)}$ be the distances respectively from \mathbf{o}_i to the center of mass of \mathcal{U}_i , and from \mathbf{j}_i to that of \mathcal{L}_i .

Clearly, the linear and angular velocities of the links \mathcal{U}_i and \mathcal{L}_i are $\mathbf{v}_i^{(u)} = h^{(u)}\dot{\theta}_i\hat{\mathbf{m}}_i^{(u)}$, $\omega_i^{(u)} = \dot{\theta}_i$, $\mathbf{v}_i^{(l)} = (\ell^{(u)}\hat{\mathbf{m}}_i^{(u)} + (1 + \varepsilon)h^{(l)}\hat{\mathbf{m}}_i^{(l)})\dot{\theta}_i$, and $\omega_i^{(l)} = (1 + \varepsilon)\dot{\theta}_i$. This leads to the kinetic energy of \mathcal{F}_i :

$$\begin{aligned} T_i &= \frac{1}{2} \left(\rho^{(u)}\omega_i^{(u)2} + \rho^{(l)}\omega_i^{(l)2} + m^{(u)}\mathbf{v}_i^{(u)2} + m^{(l)}\mathbf{v}_i^{(l)2} \right) \\ &= \frac{1}{2} \left(\rho^{(u)} + \rho^{(l)}(1 + \varepsilon)^2 + m^{(u)}h^{(u)2} + m^{(l)} \left(\ell^{(u)2} \right. \right. \\ &\quad \left. \left. + (1 + \varepsilon)^2h^{(l)2} + 2(1 + \varepsilon)\ell^{(u)}h^{(l)} \cos(\varepsilon\theta_i + \beta) \right) \right) \dot{\theta}_i^2, \end{aligned}$$

²The values of d_i and γ_i need to be calculated using the new contact vertex \mathbf{z}_j .

³defined relative to a frame attached at the center of mass of each link and aligned with $\hat{\mathbf{l}}_i$ and $\hat{\mathbf{m}}_i$ on the link.

The potential energy of the two-link system is

$$\begin{aligned} U_i &= -\mathbf{g} \cdot \left(m^{(u)}h^{(u)}\hat{\mathbf{l}}_i^{(u)} + m^{(l)} \left(\ell^{(u)}\hat{\mathbf{l}}_i^{(u)} \pm h^{(l)}\hat{\mathbf{l}}_i^{(l)} \right) \right) \\ &= - \left(m^{(u)}h^{(u)} + m^{(l)}\ell^{(u)} \right) \sin(\theta_i + \alpha) \\ &\quad \mp m^{(l)}gh^{(l)} \sin\left((1 + \varepsilon)\theta_i + \alpha + \beta \right). \end{aligned}$$

where \mathbf{g} is the gravitational acceleration vector.

The Lagrange-d'Alembert equation is in the form

$$\frac{d}{dt} \frac{\partial T_i}{\partial \dot{\theta}_i} - \frac{\partial T_i}{\partial \theta_i} + \frac{\partial U_i}{\partial \theta_i} = Q_i. \quad (43)$$

Here, Q_i is the generalized force assuming the form

$$Q_i = \tau_i - J_i^T \mathbf{f}_i. \quad (44)$$

where τ_i is the torque provided by the actuator, $-\mathbf{f}_i$ is the contact force exerted by the object, and J_i is the Jacobian for the fixed point on the link coinciding with the contact point \mathbf{p}_i given in (5):

$$J_i = \frac{\partial \mathbf{p}_i}{\partial \theta_i} = \frac{\partial (\delta_i \pm d_i \hat{\mathbf{l}}_i)}{\partial \theta_i} = \delta_i' \pm d_i \eta_i \hat{\mathbf{m}}_i,$$

with d_i treated as a constant in the above differentiation.

The Lagrange-d'Alembert equation (43) can now be rewritten as

$$M(\theta_i)\ddot{\theta}_i + C(\theta_i)\dot{\theta}_i^2 + N(\theta_i) = J_i^T(-\mathbf{f}_i) + \tau_i, \quad (45)$$

where the mass matrix and Coriolis-Centrifugal and gravity terms are given below:

$$\begin{aligned} M(\theta_i) &= \rho^{(u)} + \rho^{(l)}(1 + \varepsilon)^2 + m^{(u)}h^{(u)2} + m^{(l)} \cdot \\ &\quad \left(\ell^{(u)2} + \varepsilon^2h^{(l)2} + 2\varepsilon h^{(l)}\ell^{(u)} \cos(\varepsilon\theta_i + \beta) \right), \\ C(\theta_i) &= -\varepsilon(1 + \varepsilon)m^{(l)}h^{(l)}\ell^{(u)} \sin(\varepsilon\theta_i + \beta), \\ N(\theta_i) &= -(m^{(u)}h^{(u)} + m^{(l)}\ell^{(u)})g \cos(\theta_i + \alpha) \\ &\quad \mp (1 + \varepsilon)m^{(l)}h^{(l)}g \cos\left((1 + \varepsilon)\theta_i + \alpha + \beta \right). \end{aligned}$$

B. Hand Dynamics

For $i = 1, 2$ we denote $M_i = M(\theta_i)$, $C_i = C(\theta_i)$, and $N_i = N(\theta_i)$. Also, let $\boldsymbol{\tau} = (\tau_1, \tau_2)^T$. We combine the dynamics (45) of the two fingers:

$$\boldsymbol{\tau} = \begin{pmatrix} M_1 & 0 \\ 0 & M_2 \end{pmatrix} \ddot{\boldsymbol{\theta}} + \begin{pmatrix} C_1 \dot{\theta}_1^2 \\ C_2 \dot{\theta}_2^2 \end{pmatrix} + \begin{pmatrix} N_1 \\ N_2 \end{pmatrix} + \begin{pmatrix} J_1^T \mathbf{f}_1 \\ J_2^T \mathbf{f}_2 \end{pmatrix}. \quad (46)$$

If both contacts are sliding, then \mathbf{f}_1 and \mathbf{f}_2 are given in (19). Introduce a diagonal matrix $F =$

diag($J_1^T \mathbf{w}_1, J_2^T \mathbf{w}_2$). Apply (23) to transform (46) into

$$\begin{aligned} \boldsymbol{\tau} = & \left[\begin{pmatrix} M_1 & 0 \\ 0 & M_2 \end{pmatrix} + FK \right] \ddot{\boldsymbol{\theta}} + \left[\begin{pmatrix} C_1 \dot{\theta}_1^2 \\ C_2 \dot{\theta}_2^2 \end{pmatrix} + F\mathbf{k}_1 \right] \\ & + \left[\begin{pmatrix} N_1 \\ N_2 \end{pmatrix} + F\mathbf{k}_2 \right] \end{aligned} \quad (47)$$

$$= \mathcal{M}(\boldsymbol{\zeta})\ddot{\boldsymbol{\phi}} + \mathcal{C}(\boldsymbol{\zeta}, \dot{\boldsymbol{\phi}}) + \mathcal{N}(\boldsymbol{\phi}), \quad (48)$$

where $\mathcal{M}, \mathcal{C}, \mathcal{N}$ are via a comparison with (47). If the contact \mathbf{p}_i is rolling (and therefore the contact $\mathbf{p}_j, j \neq i$, must be sliding), we plug (41) into (46):

$$\begin{aligned} \begin{pmatrix} \tau_i \\ \tau_j \end{pmatrix} = & \left[\begin{pmatrix} M_i & 0 \\ 0 & M_j \end{pmatrix} + \begin{pmatrix} J_i^T B_i \\ J_j^T B_j \end{pmatrix} \right] \begin{pmatrix} \ddot{\theta}_i \\ \ddot{\theta}_j \end{pmatrix} + \\ & \left[\begin{pmatrix} C_i \dot{\theta}_i^2 \\ C_j \dot{\theta}_j^2 \end{pmatrix} + \begin{pmatrix} J_i^T \mathbf{s}_i \\ J_j^T \mathbf{s}_j \end{pmatrix} \right] + \left[\begin{pmatrix} N_i \\ N_j \end{pmatrix} + \begin{pmatrix} J_i^T \mathbf{t}_i \\ J_j^T \mathbf{t}_j \end{pmatrix} \right]. \end{aligned} \quad (49)$$

As the contact mode changes, the hand dynamics switch between (47) and (49). When both contact are sliding, check constantly if the condition $\mathbf{v}_i^{(o)} = \mathbf{v}_i^{(f)}$ holds for either $i = 1$ or 2 . If so, rolling starts at the contact \mathbf{p}_i . Similarly, suppose rolling happens at the contact \mathbf{p}_i . As soon as the contact force \mathbf{f}_i reaches the edge of the contact friction cone, sliding starts at \mathbf{p}_i .

At the start of manipulation, we need to hypothesize three possibilities: sliding at both \mathbf{p}_1 and \mathbf{p}_2 , rolling at \mathbf{p}_1 only, and rolling at \mathbf{p}_2 only. Apply the corresponding dynamics with $\boldsymbol{\tau}$ and check if the contact force or velocity is consistent with the hypothesis.

VI. CONTROL AND PLANNING

The manipulation task is to move the object with an initial state $\zeta_0 = (\mathbf{c}_0, \psi_0)$ to some goal state $\zeta_d = (\mathbf{c}_d, \psi_d)$. First, we look at how to achieve the target position \mathbf{c}_d . Using inverse kinematics, we obtain the desired values $\boldsymbol{\theta}_d$ of the joint angles with $\dot{\boldsymbol{\theta}}_d = \mathbf{0}$ and $\ddot{\boldsymbol{\theta}}_d = \mathbf{0}$. Let $\boldsymbol{\theta}_e = \boldsymbol{\theta} - \boldsymbol{\theta}_d$. In the case of both contacts sliding, we apply the following proportional-derivative (PD) control law from [11, p. 191]:

$$\boldsymbol{\tau} = \mathcal{M}(\ddot{\boldsymbol{\theta}}_d - K_v \dot{\boldsymbol{\theta}}_e - K_p \boldsymbol{\theta}_e) + \mathcal{C} + \mathcal{N}. \quad (50)$$

Substitution of the above into (48) yields

$$\mathcal{M}(\ddot{\boldsymbol{\theta}}_e + K_v \dot{\boldsymbol{\theta}}_e + K_p \boldsymbol{\theta}_e) = \mathbf{0}.$$

which, given the positive definiteness of \mathcal{M} , leads to the following error dynamics:

$$\ddot{\boldsymbol{\theta}}_e + K_v \dot{\boldsymbol{\theta}}_e + K_p \boldsymbol{\theta}_e = \mathbf{0}. \quad (51)$$

With $K_v = k_v I_2$ and $K_e = k_e I_2$ for some $k_v, k_e > 0$, the error $\boldsymbol{\theta}_e$ will go down exponentially to zero as sliding continues.

Similarly, the error dynamics for rolling at \mathbf{p}_i while sliding at \mathbf{p}_j are derived as

$$\ddot{\phi}_e + K_v \dot{\phi}_e + K_p \phi_e = \mathbf{0}. \quad (52)$$

Again, the error ϕ_e will go down exponentially if no contact mode changes.

Under the error dynamics (51) and (52), the targeted joint angles $\boldsymbol{\theta}_d$ will be reached and the object is expected to be at the target location, unless one of the joint angles, velocities, or accelerations goes out of its range. To simultaneously reach the target orientation ψ_0 , we need to choose proper values for K_v and K_p . Here is a simple strategy. Start with some random value for the pair (K_v, K_p) , and use the error dynamics to compute the deviation $\psi - \psi_d$ when $\boldsymbol{\theta}$ tends to $\boldsymbol{\theta}_d$. Repeat until two values (K_v^-, K_p^-) and (K_v^+, K_p^+) are found to yield negative and positive deviations, respectively. Then use bisection with the gain $\lambda(K_v^-, K_p^-) + (1 - \lambda)(K_v^+, K_p^+)$ over $[0, 1]$ to find a value that achieves $\psi = \psi_d$.

VII. SIMULATION

The two fingers in the simulation use the mass and inertia properties of those of the Barrett Hand BH8-282 [1]. We apply the error dynamics (51) or (52) to generate the trajectory of $\boldsymbol{\theta}_e(t)$. The trajectories $\boldsymbol{\theta}(t), \dot{\boldsymbol{\theta}}(t), \ddot{\boldsymbol{\theta}}(t)$ of the joint angles, velocities, and accelerations are determined along the way. The object's orientation ψ is tracked via numerical integration, so are the contact modes. The center of mass \mathbf{c} is determined from (7). All units are from the metric system.

Fig. 2 shows several snapshots of a hand manipulating a disk of radius 0.03. The coefficient of contact

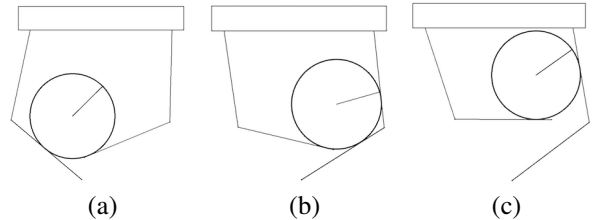


Fig. 2. Snapshots of manipulating a disk taken at the (a) start (0.0 s), (b) transition of contact on the right finger \mathcal{F}_2 (0.3727 s), and (c) end (0.93 s). The hand parameter values are: $\ell^{(u)} = \ell^{(l)} = 0.065$, $\|\mathbf{o}_1 - \mathbf{o}_2\| = 0.05$, $\alpha = 0.428$, and $\beta = 0.656$.

friction is $\mu = 0.2$. Initially, the disk is located at $\mathbf{c}_0 = (-0.02, -0.13)^T$ at the orientation $\psi_0 = 0$. It needs to be transferred to $\mathbf{c}_d = (0.025, -0.1)^T$ while rotated through -0.151 . The manipulation lasted 0.93 s using the gain values $K_p = 36$ and $K_v = 12$. Fig. 3 plots the (blue) trajectory of the circle during the manipulation. The movements by the contact points

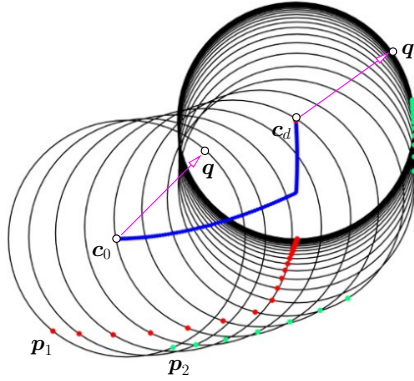


Fig. 3. Trajectories of the circle and the two contact points during the manipulation illustrated in Fig. 2.

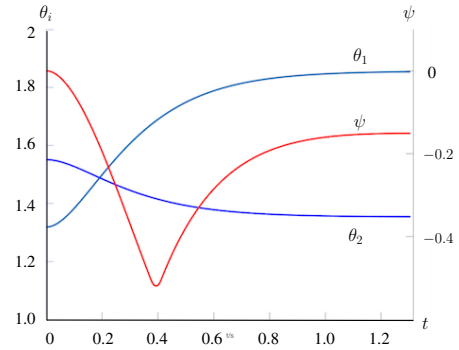
p_1 and p_2 are represented by two sequences of points (red and green, respectively). The circle's change in orientation is represented by the vector from the center of mass c to the point q initially with polar angle $\frac{\pi}{4}$. Fig. 4 displays the trajectories of the joint angles and the object's orientation, as well as of the applied joint torques. We see that the object started with a clockwise rotation (achieving a minimum of -0.519) and later changed to a counterclockwise rotation. It reached the target orientation very early but had to continue the rotation in order to move to the target location.

Fig. 5 shows the manipulation of a concave 6-gon with a duration of 1.5 s. Let S and R denote sliding and rolling contacts, respectively. The two contacts p_1 and p_2 have sequentially experienced six pairs of modes: $\langle S, S \rangle$, $\langle S, R \rangle$, $\langle S, S \rangle$, $\langle R, S \rangle$, $\langle S, S \rangle$, and $\langle S, R \rangle$ with transitions happening at 0.010 s, 0.170 s, 0.193 s, 0.788 s, and 0.790 s, respectively. No reverse sliding has happened to either contact. Part (a) of Fig. 6 displays the joint angle trajectories as well as the trajectory of the object's orientation, and part (b) displays the torque trajectories.

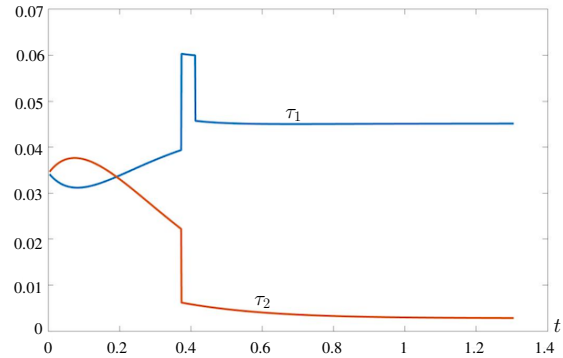
VIII. DISCUSSION

The object may be in contact with the endpoint of a lower link. In this case, a new form of c can be derived to replace (7), and contact kinematics use the object's normal instead of the link normal. Add two new hand dynamics equations like (47) and (49) (for different combinations of contact modes).

We also need some understanding about the conditions over the gains K_p and K_d that will result in a successful maneuver. More importantly, we would like to characterize the range of final poses that are achievable under kinematic constraints and influenced by the object geometry. The manipulation strategy then



(a)



(b)

Fig. 4. Trajectories during the manipulation in Fig. 3: (a) joint angles and the object's orientation, and (b) joint torques.

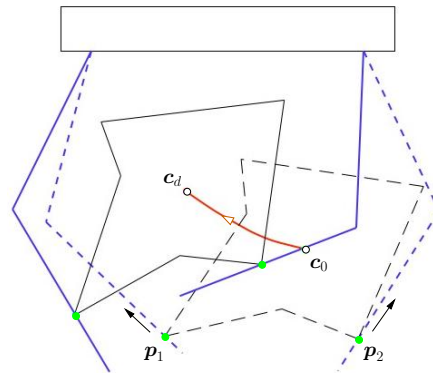


Fig. 5. Manipulation of a 6-gon from an initial pose (in dashed lines) to the desired pose (in solid lines). Here, $\psi_0 = 0$, $c_0 = (0.01, -0.14383)^T$, and $c_d = (-0.015, -0.12038)^T$. Physical parameters: $m = 0.14384$ kg, $\rho = 9.84914 \cdot 10^{-5}$ kg m², mass density 40 kg/m², and $\mu = 0.7$. Control gains: $k_p = 100$ and $k_v = 20$.

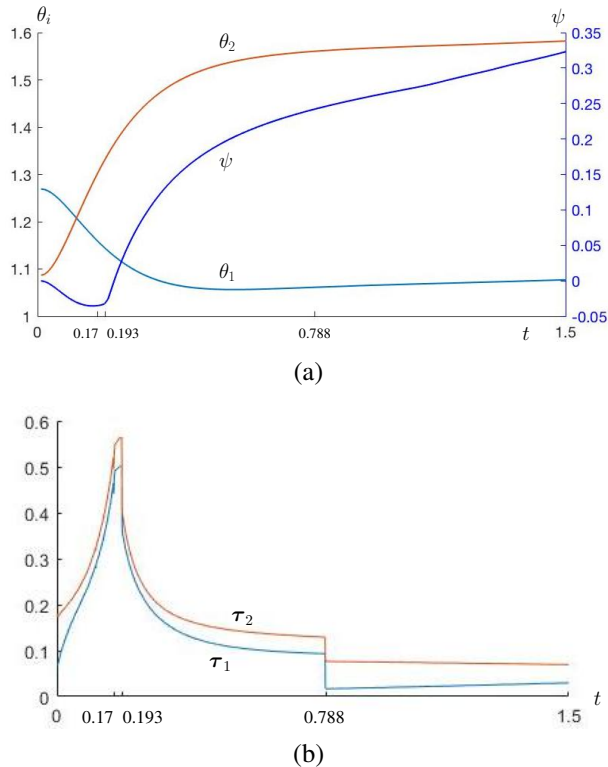


Fig. 6. (a) Joint and orientation trajectories during the manipulation of the 6-gon in Fig. 5. (b) Torque trajectories.

should be extended to include initial grasp achievement with gravity taken into account.

The presented work does not cope with uncertainties. Torque control usually has delays to make it less effective, hand dynamics are unlikely to be accurate sometimes due to joint friction, and contact friction with the object may vary during sliding. The effects of these uncertainties on the performance of the control law need to be investigated for improvement.

The next step is experimental validation with the Barrett Hand, to which the hand dynamics derived in Section V carry over to only the period before contact establishment. An extension to the period with contact engagement needs to be done. Several other issues will have to be addressed: finger contact modeling, contact kinematics for three fingers with 4DOFs (including one for palm spreading), and inverse kinematics. Our longer term objective is to tackle challenging control and planning issues in a grasping and/or reorienting task, which may be dissected into a sequence of states with transitions implemented by finger gaiting. One example is to pick up a kitchen knife and rotate it to the vertical position so it becomes ready for cutting.

IX. ACKNOWLEDGMENT

We would like to thank Xiaoqian Mu for her help with the simulation, as well as the anonymous reviewers for their valuable feedback. Support for this research has been provided by the US National Science Foundation under Grant IIS-1651792. Any opinions, findings, and conclusions or recommendations expressed in this material are those of the authors and do not necessarily reflect the views of the National Science Foundation.

REFERENCES

- [1] Barrett Technology, LLC. <http://support.barrett.com/wiki/Hand/282/MassProperties>. *Inertial Tensors and Mass Properties for the BarrettHand BH8-282*. Also, <http://support.barrett.com/wiki/Hand/280/KinematicsJointRangesConversionFactors>. *BarrettHand BH8-280/282 Kinematics, Joint Ranges, Conversion Factors*.
- [2] A. Bicchi. Hands for dexterous manipulation and robust grasping: a difficult road toward simplicity. *IEEE Trans. Robot. Autom.*, vol. 16, no. 6, pp. 652–662, 2000.
- [3] M. Cherif and K. K. Gupta. Global planning for dexterous reorientation of rigid objects: finger tracking with rolling and sliding. *Int. J. Robot. Res.*, vol. 20, no. 1, pp. 57–84, 2001.
- [4] A. A. Cole, P. Hsu, and S. S. Sastry. Dynamic control of sliding by robot hands for regrasping. *IEEE Trans. Robot. Autom.*, vol. 8, no. 1, pp. 42–52, 1992.
- [5] A. A. Cole, P. Hsu, and S. S. Sastry. Kinematics and control of multifingered hands with rolling contact. *IEEE Trans. Autom. Control*, vol. 34, no. 4, pp. 398–404, 1989.
- [6] Aaron M. Dollar and Robert D. Howe. The highly adaptive SDM hand: design and performance evaluation. *Int. J. Robot. Res.*, vol. 29, no. 5, pp. 585–597, 2010.
- [7] M. R. Hasan, R. Vepa, H. Shaheed, and H. Hujiberts. Modeling and control of the Barrett Hand for grasping. In *Proc. 15th Int. Conf. Computer Model. Simul.*, pp. 230–234, 2013.
- [8] S. C. Jacobsen, E. K. Iversen, D. F. Knutti, R. T. Johnson, and K. B. Biggers. Design of the Utah/MIT dextrous hand. In *Proc. IEEE Int. Conf. Robot. Autom.*, pp. 1520–1532, 1986.
- [9] Y.-B. Jia and F. Wang. Analysis and computation of two body impact in three dimensions. *ASME J. Comp. Nonlinear Dynamics*, vol. 12, no. 4, pp. 04012-1, 2017. in press.
- [10] I. Kao and M. R. Cutkosky. Comparison of theoretical and experimental force/motion trajectories for dextrous manipulation with sliding. *Int. J. Robot. Res.*, vol. 12, no. 6, pp. 529–534, 1993.
- [11] R. M. Murray, Z. Li, and S. S. Sastry. *A Mathematical Introduction to Robotic Manipulation*. CRC Press, Boca Raton, FL, 1994.
- [12] M. Reichel. Transformation of Shadow dextrous hand and Shadow finger test unit from prototype to product for intelligent manipulation and grasping. In *Proc. Int. Conf. Intell. Manipulation Grasping*, 2004.
- [13] J. K. Salisbury and J. J. Craig. Articulated hands: force control and kinematic issues. *Int. J. Robot. Res.*, vol. 1, no. 1, pp. 4–17, 1982.
- [14] W. T. Townsend. The Barrett Hand grasper — programmably flexible part handling and assembly. *Industrial Robot: An Int. J.*, vol. 10, no. 3, pp. 181–188, 2000.
- [15] J. C. Trinkle and R. P. Paul. Planning for dexterous manipulation with sliding contacts. *Int. J. Robot. Res.*, vol. 9, no. 3, pp. 24–48, 1990.